cells, see G. A. Somorjai, *Chemistry in Two Dimensions: Surfaces* (Cornell Univ. Press, Ithaca, NY, 1981).
18. J. Y. Katekaru, G. A. Garwood, Jr., J. Hershberger, A. T. Hubbard, *Surf. Sci.* **121**, 396 (1982).
19. D. Zurawski, L. Rice, M. Hourani, A. Wieckowski, *J. Electroanal. Chem.* **230**, 221 (1987).
20. A. Wieckowski, S. D. Rosasco, B. C. Schardt, J. L. Stickney, A. T. Hubbard, *Inorg. Chem.* **23**, 565 (1984).
21. The Pt(111) single crystal disk was obtained from Johnson Matthey. Laue back-reflection x-ray photography was used to determine that the crystal was properly oriented within 0.5°. The Laue results were used to scribe a mark on the side and back face of the crystal to indicate the Pt substrate unit cell orientation.
22. The maximum scan range of the microscope head in both the x and y axes was 600 nm. All of the images shown were obtained in the constant height, fast-scan mode of the STM [A. Bryant, D. P. E. Smith, C. F. Quate, *Appl. Phys. Lett.* **48**, 832 (1986)]. The x-axis raster frequency was 156 Hz, with 200 or 400 scan lines per image. The images reported have had a least-squares plane subtracted to remove any tilt of the microscope head relative to the sample surface. Images are presented as a gray scale proportional to the natural logarithm of the measured tunneling current; the measured current increases from black to white. The tunneling probe tips were made from tungsten wire, 0.025 cm in diameter, etched in 1*M* KOH at 10 V and 60 Hz ac.
23. Supported by the Industrial Associates program at Purdue University funded in part by Dow Chemical Co. and BP America, and a Basic Research Grant from Chevron Research Company.

6 December 1988; accepted 28 December 1988

Uranium-Series Dated Authigenic Carbonates and Acheulian Sites in Southern Egypt

B. J. Szabo, W. P. McHugh, G. G. Schaber, C. V. Haynes, Jr., C. S. Breed

Field investigations in southern Egypt have yielded Acheulian artifacts in situ in authigenic carbonate deposits ($CaCO_3$-cemented alluvium) along the edges of now-aggraded paleovalleys (Wadi Arid and Wadi Safsaf). Uranium-series dating of 25 carbonate samples from various localities as far apart as 70 kilometers indicates that widespread carbonate deposition occurred about 45, 141 and 212 ka (thousand years ago). Most of the carbonate appears to have been precipitated from groundwater, which suggests that these three episodes of deposition may be related to late Pleistocene humid climates that facilitated human settlement in this now hyperarid region. Carbonate cements from sediments containing Acheulian artifacts provide a minimum age of 212 ka for early occupation of the paleovalleys.

The area west of the Nile (Fig. 1) is barren of human occupation and is one of the most arid regions on earth. However, aggraded paleovalleys, parts of ancient drainage systems, have been identified recently through the use of space shuttle imaging radar (SIR) (*1, 2*). During subsequent field expeditions to investigate the radar geology of these paleovalleys (*2–4*), we discovered many Acheulian (lower Paleolithic) sites both on the surface and buried in alluvium along the edges of several of these features. The sedimentary contexts of the buried Acheulian sites indicate that the groundwater table was shallow during periods of Acheulian occupation. Extensive carbonate (calcrete) was deposited by this ground water, ultimately cementing the alluvial sand and gravel and some of the artifacts. In this report, we present uranium-series (U-series) dates of this authigenic carbonate that provide a preliminary basis for dating episodes of carbonate deposition, pluvial climatic phases, and artifacts incorporated in the sediments relating to the settlement of the area by early man.

Archeological sites, especially Holocene-age Neolithic sites, are abundant along the edges of the ancient valleys and in the intervening interfluves (*5*); they provide evidence of a long but discontinuous occupation of this region. Geoarchaeological evidence indicates that there were several episodes of climatic and cultural change in the region since the last stages of valley aggradation more than 0.2 million years ago (*6*).

We have studied two of the radar valleys (wadis) in the heart of the hyperarid Eastern Sahara (Fig. 1): Wadi Arid ("wide wadi," about 15 km wide, 100 km long, and 350 km west of Lake Nasser) and Wadi Safsaf (including Bir Safsar, about 70 km northeast of Wadi Arid). Seismic data indicate that Wadi Arid is filled by several hundred meters of sediment above bedrock (*7*). A series of braided channels, possibly Holocene, is inset into the large Safsaf valley (*3*). A bedrock divide covered by sand sheet deposits is thought to separate Wadi Safsaf from Wadi Arid (*2, 6*). The upper parts of the valley fill of both Wadi Arid and Wadi Safsaf consist of sand and small gravel alluvium below a thin sand cover that is transparent to the SIR sensor (*1, 3*).

In 10 of 36 backhoe trenches (BHTs) along the southeast edge of Wadi Arid (Fig. 2) we found artifacts at depths of 1 to 3 m; three BHTs yielded hand axes, the diagnostic Acheulian artifact. Only one BHT in the middle of the wadi yielded artifacts. Along the northwest margin of the wadi, the upper part of the valley fill has been eroded away exposing a strongly carbonate-cemented terrace (Fig. 2) on which several Acheulian sites were found. Test pits dug in this terrace (site 84F21-7) yielded handaxes and other artifacts at shallow depths (to 50 cm), including four large middle Acheulian hand axes from a loose, noncemented sheetwash deposit (*8*).

Backhoe excavations in Wadi Safsaf allowed the determination of the features in the filled inset channels and the valley fill (*3*) that were responsible for the SIR images, but they yielded no artifacts from strata that could be dated accurately. In addition to the many Neolithic sites among the braided channels, we found few middle Paleolithic sites in the area and some extensive Acheulian sites around the perimeter of Bir Safsaf (*6, 8*) and in a depression south of Wadi Safsaf. Brief investigation of one of these sites southeast of Bir Safsaf yielded two late Acheulian (*6, 8*) hand axes in situ in a loose, carbonate-impregnated sandy matrix.

The bedrock bordering Wadi Arid and Wadi Safsaf is mostly quartzitic sandstone that contains no calcium carbonate (*9*). The source of the calcium in the secondary calcite may be airborne dust that was transported from the Eocene limestone plateau northeast of the radar valleys (Fig. 1). The processes involved in the carbonate cementation of the valley fill are not yet clear. McCauley *et al.* (*2*) and Haynes (*10*) have concluded that most secondary carbonate deposits (calcretes, nodules, and carbonate cements in

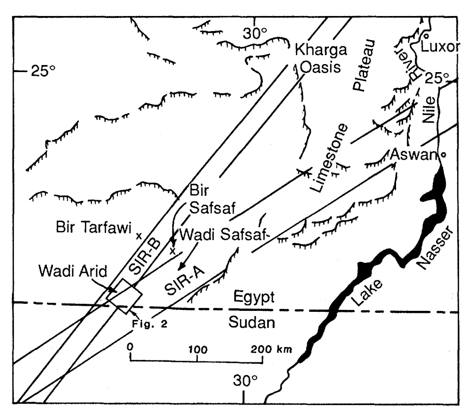

Fig. 1. Map showing location of paleovalley study areas and SIR groundtracks in southern Egypt.

B. J. Szabo, U.S. Geological Survey, Box 25046, Mail Stop 963, Denver, CO 80225.
W. P. McHugh, EPIX Incorporated; 571 Coal Street, Wilkinsburg, PA 15221.
G. G. Schaber and C. S. Breed, U.S. Geological Survey, 2255 North Gemini Drive, Flagstaff, AZ 86001.
C. V. Haynes, Department of Anthropology, University of Arizona, Tucson, AZ 85721.

the calichified alluvium) in southwestern Egypt were precipitated in shallow groundwater environments. Calichified rootcasts have a different origin, possibly forming in the vadose zone. Except for sample VH-7 (Table 1), there is little evidence for pedogenic carbonate deposits due to repeated deflation of the sediment surface.

We collected carbonate samples for U-series dating from surface calcretes, rootcasts, trench walls, and cemented sediments, some of which adhered to artifacts (*11*). The carbonate samples analyzed fall into three age groups (Fig. 3) with averages of about 45, 141, and 212 ka. One sample (Sch-3) yielded a corrected age of 15 ± 2 ka, and another sample (Sch-1) had an age older than 300 ka. Only sample Sch-18L yielded a $^{230}Th/^{232}Th$ ratio high enough (68 ± 8) that it did not require correction for initial Th and U of detrital origin. The calculated age (152 ± 9 ka) of this sample is concordant with the average group age of 141 ± 7 ka obtained for other samples with the isochron-plot correction. By running duplicate and triplicate analyses, we learned that some Th of the leachate was absorbed by the residue fraction during the acid leaching and during separation of acid-soluble and acid-insoluble fractions. For these replicate analyses, we plotted the highest value of the ratio of ^{230}Th to ^{234}U for a given sample (Table 1) in Fig. 3 to avoid underestimating the calculated ages. Exchange or precipitation of younger pedogenic carbonate with the dated carbonate may also result in ages that are younger than most of the $CaCO_3$ deposition. That the isotopic data (Table 2 and Fig. 3) from samples taken a few hundred meters to as much as 70 km apart cluster along a few isochrons suggests that the average group ages are reasonable, although possibly minimum, estimates of the periods of significant carbonate deposition in the study area.

Table 1. Location, description, concentration, and activity ratio data of carbonates from southern Egypt (group by age).

Sample	Location and description*	Percent acid-insoluble fraction (weight percent)	Uranium† (ppm)	Activity ratios†		
				$^{234}U/^{238}U$	$^{230}Th/^{232}Th$	$^{230}Th/^{234}U$
			15 ka			
Sch-3	WS; T84-60; rc	7	0.589(12)	1.010(14)	4.36(36)	0.150(5)
			45 ka			
Sch-2	WS; T84-60; cn	8	0.453(10)	0.998(16)	2.99(9)	0.458(11)
Sch-4	WS; rc	4	0.740(15)	1.024(14)	7.83(54)	0.372(9)
Sch-20	WS; cal	12	0.667(14)	1.032(16)	4.64(21)	0.307(7)
Sch-19	BT; cp	11	0.556(11)	1.052(15)	5.67(19)	0.426(9)
Sch-5	WA; T84-27; pg	67	4.14(8)	0.952(11)	1.58(2)	0.713(15)
Sch-5R‡			1.64(3)	0.980(12)	0.635(11)	1.30(6)
Sch-7	WA; T84-3; cal	26	2.65(5)	0.994(12)	9.69(23)	0.360(7)
VH-3	WA; T84-10:110; cn	21	0.675(14)	0.913(13)	1.74(6)	0.588(17)
VH-4A	WA; T85-70:144; cc	37	1.04(2)	0.920(12)	2.0(4)	0.65(14)§
VH-4B		34	0.880(20)	1.047(18)	1.65(6)	0.596(22)
			141 ka			
Sch-6	WA; T84-25; ca	7	1.07(2)	0.971(12)	3.29(7)	0.781(16)
Sch-6R‡			1.67(4)	0.936(21)	0.654(12)	1.46(7)
Sch-11A	WS; T85-10; cf	27	1.14(2)	1.028(13)	2.25(3)	0.778(15)§
Sch-11B		28	1.16(2)	1.056(15)	1.29(4)	0.734(15)
Sch-11L‖		33	1.01(2)	1.021(21)	3.14(10)	0.689(18)§
VH-1	WA; T84-10:114; cn	22	0.913(33)	0.971(13)	2.22(4)	0.807(17)
Sch-16	WA; T84-23; cala	40	1.72(4)	1.002(20)	1.21(3)	0.755(21)
Sch-17	WA; T84-1; cala	32	1.63(4)	1.032(18)	1.87(4)	0.734(17)
Sch-18A	WS; rc	11	1.88(4)	0.966(12)	6.43(13)	0.649(12)
Sch-18L‖		14	1.83(4)	1.010(16)	68(8)	0.756(18)§
Sch-18R‡			1.44(6)	1.048(28)	0.787(19)	1.89(9)
VH-5A	WA; T84-3:69; cal	19	2.00(4)	0.987(11)	5.06(11)	0.640(16)
VH-5B	do.	17	1.93(4)	1.001(12)	5.81(12)	0.773(17)
VH-5L‖	do.	24	1.97(5)	1.000(15)	9.35(30)	0.680(16)§
			<180 ka			
VH-7	WA; T84-7:93; cal	13	0.387(8)	0.988(13)	0.424(9)	0.857(20)§
			212 ka			
Sch-15A	BS; cala	13	1.68(3)	1.093(13)	3.62(12)	0.906(29)
Sch-15B		14	1.74(4)	1.103(16)	4.38(11)	0.905(21)
Sch-15L‖		19	1.23(2)	1.116(4)	9.15(36)	0.398(8)
Sch-12B	WA; T84-10; cf	31	0.553(12)	1.014(14)	1.51(3)	0.794(18)§
Sch-12L‖		34	0.503(13)	1.064(24)	2.67(8)	0.813(24)
Sch-13	WA; P84-11:SF21-7; cf	26	2.07(4)	0.986(12)	4.06(11)	0.940(45)
Sch-14A	WA; P84-5:SF21-7; cf	33	2.48(5)	0.983(13)	3.50(14)	0.792(25)§
Sch-14B	do.	31	2.32(5)	1.036(15)	3.75(7)	0.887(18)
VH-2	WA; T84-10:117; cf	25	3.45(7)	0.945(12)	5.91(13)	0.899(27)
VH-10	WA; T84-10:117; cn	30	0.627(12)	1.024(12)	3.27(6)	0.855(16)
VH-6A	WA; T84-3:70; cal	28	2.42(5)	0.961(12)	3.76(12)	0.802(28)§
VH-6B		29	2.33(5)	0.978(12)	4.50(9)	0.909(20)
VH-6L‖		34	2.37(5)	0.963(15)	7.12(26)	0.634(16)
			>300 ka			
Sch-1	WA; T84-28; cal	28	1.47(3)	0.987(12)	3.20(7)	0.998(26)
Sch-1R‡			1.17(2)	0.932(14)	0.530(12)	1.01(3)

*Abbreviations: WA, Wadi Arid; WS, Wadi Safsaf; BT, Bir Tarfawi; BS, Bir Safsaf; T, backhoe trench; P, test pit; S, site; rc, rootcast; cn, carbonate nodule; cal, calcrete; cp, carbonate platform; cpg, calichified pea gravel; cc, carbonate crust; ca, carbonate accumulation; cf, carbonate on flake; cala, calichified alluvium. †Errors of activity ratios and U (in parentheses) represent 1 SD of propagated error, components of which include counting statistics on single nuclide measurements, errors due to data manipulations, errors on background corrections, and errors associated with reference control. ‡Acid-insoluble residue. §Not included in final isochron plots. ‖Unheated carbonate sample; acid-insoluble residue and acid-soluble carbonate fraction were separated by dilute HNO_3 leaching.

By the beginning of the period given by the carbonate dates (>300 to 141 ka ago), the broad valleys were already aggraded to or above current elevations. The last phases of aggradation buried the earlier Acheulian artifacts. During episodes of carbonate deposition, groundwater conditions were such that the water-table and capillary-fringe fluctuations, which would be where carbonate precipitates, were fairly shallow. The U-series group ages indicate that such humid conditions occurred around >300, 212, 141, 45, and possibly 15 ka.

In contrast, modern yearly precipitation in the core of the Eastern Sahara is less than 1 mm, and groundwater levels, except in widely scattered localities, are tens of meters below the surface. Significant diagenetic or pedogenic carbonate deposition therefore cannot occur. According to Goudie and Pye (*12*), diagenetic carbonates form only in areas where average annual rainfall is between 175 mm and 600 mm.

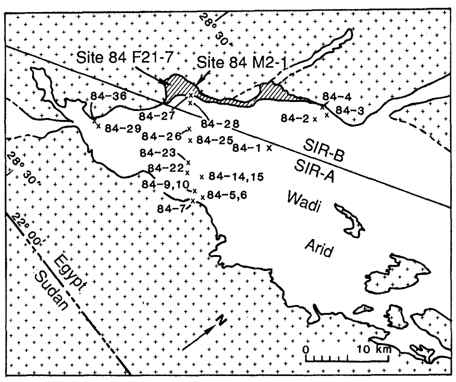

Fig. 2. Drawing made from composite radar coverage (SIR-A and SIR-B) of Wadi Arid study area showing locations of backhoe trenches (number 84 followed by numbers). Test pits 5 and 11 were dug at site 84F21-7. Many Acheulian sites are exposed on the wadi surface or are buried in the carbonate-cemented gravels. Hachures indicate radar-bright, truncated, carbonate-cemented terrace along the edge of wadi. Stippled areas are bright on SIR images; white area is radar dark; dashed lines between areas indicate inferred contacts.

The assigned dates in BHTs 3, 10, and 27 (Table 1) are stratigraphically inverted, that is, the lowest sample is the youngest. These inversions may be a result of decreasing maximum water-table levels during Pleistocene pluvials, where older carbonate, lying above subsequent water-table levels, were partially or wholly dissolved and replaced by younger carbonate (*12*). During the carbonate forming event at ~212 ka, the groundwater level was evidently high in most places; water during the events at 141 and 45 ka apparently did not reach such a high level. There are, however, some exceptions: in BHT 84-10 (Fig. 2), 212-ka carbonate (sample VH-2) lies between 45- (sample VH-3) and 141-ka carbonate (sample VH-1) (*13*).

Geoarcheological relations and the carbonate dates (*6*) indicate that following a very long period (Miocene to middle Pleistocene) of presumably intermittent aggradation of the radar valleys, middle (?) to late Acheulian hominids settled the valley edges during the final major episode of aggradation. Following a hiatus in deposition and an arid interval, late Acheulian hominids occupied both Wadi Arid and Wadi Safsaf as the last extensive aggradation took place. After a long arid interval, middle Paleolithic groups appeared; their sites are less common than the late Acheulian sites and are not restricted to the valley edges as are the earlier sites. Another long arid interval followed before the earliest terminal Paleolithic or Neolithic groups appeared toward the end of the Pleistocene or during the early Holocene.

The most significant ages for dating the times of human occupation are those on

Table 2. Distribution of dated carbonates by modal age and locality.

Modal ages (ka)	15 ±2	45 ±2	141 ±7	<180	212 ±18	>300
Wadi Arid		6	11	1	10	2
Wadi-Bir Safsaf	1	3	3		3	
Bir Tarfawi		1				
Total*	1	10	14	1	13	2

*The 41 analyses (including acid-insoluble residues) were run on 25 samples from 18 provenence units: 12 in Wadi Arid, 5 in Wadi Safsaf and Bir Safsaf, and 1 in Bir Tarfawi.

carbonates from BHT 84-10 and its extension, at the southeast edge of Wadi Arid, and from test pits 5 and 11 in Site 84F21-7, northwest edge of Wadi Arid. Trench BHT 84-10 and its extension yielded a large core stone, several dozen flakes, and seven handaxes, all of which we tentatively assigned to a stage earlier than that of the late Acheulian (*6, 8*). Similarly, test pits in site 84F21-7 yielded flakes and a few coarse handaxes that we also considered to be earlier than late Acheulian. Four carbonate samples from BHT 84-10 and site 84F21-7 (samples Sch-12, -13, -14, and VH-2 in Table 1) were dated as 212 ka. Another carbonate sample from sediment cemented to a flake (Sch-11 from BHT 84-10) yielded a date of 141 ka. A date of 141 ka was also obtained for samples from three other units in Wadi Arid and one in Wadi Safsaf, and thus it appears to be a reliable modal date.

The dates on carbonates adhering to artifacts provide minimum age estimates for the artifacts because the carbonate deposits are secondary. Therefore, the in situ Acheulian artifacts should be more than 212 ka old; these were typically covered by 0.5 to 1.0 m (or more) of alluvium. Deposition clearly continued after an earlier stage of late Acheulian occupation (*8*). Because late Acheulian

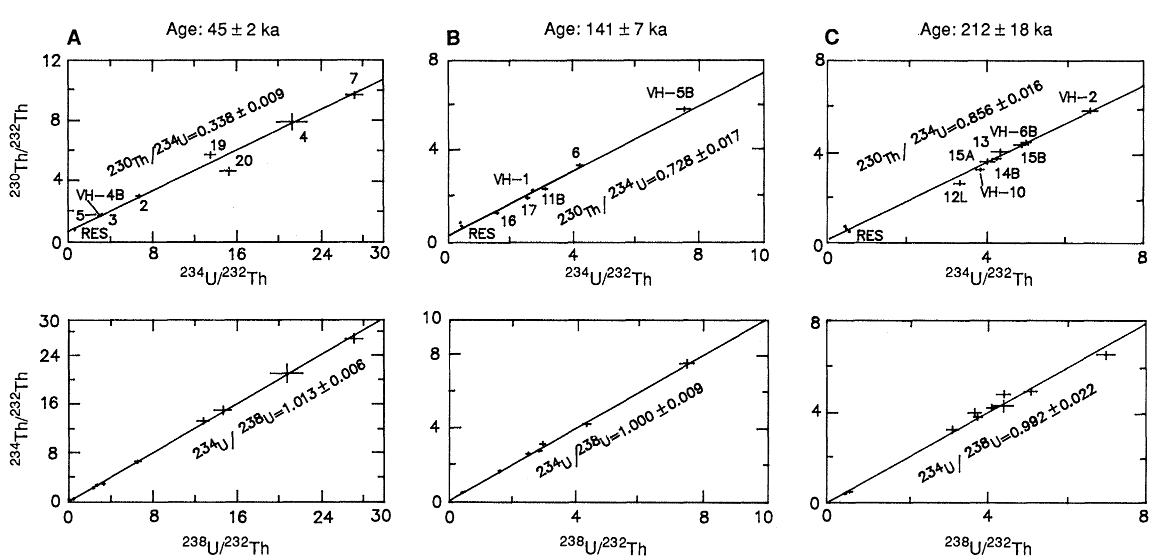

Fig. 3. Chronographs showing plots of isotope ratios used to correct for acid-leaching effect of dated authigenic carbonates (*11*). Error bars indicate 1 SD analytical uncertainties (Table 1); lines were obtained by least-squares fitting. The slopes of the lines are the detritus-corrected $^{230}Th/^{234}U$ and $^{234}U/^{238}U$ activity ratios. From these values, the average U-series group ages are calculated from half-lives of ^{230}Th and ^{234}U of 72,200 and 244,000 years, respectively.

hand axes have been observed protruding from or lying directly on near-surface calichified alluvium, we believe that some late Acheulian occupations were contemporary with the last stages of aggradation along the edges of the large valleys, perhaps as late as 141 ka. At Bir Tarfawi (Fig. 1), late Acheulian remains are associated with lake beds and spring deposits inset into a broad, carbonate-cemented plain that bears many Acheulian sites (*14*). These carbonate deposits and Acheulian sites are most likely penecontemporaneous with those in Wadi Arid.

Middle Paleolithic artifacts are indirectly associated with the third carbonate deposition episode at 45 ka; they occur in freshwater deposits, and similar deposits (containing the bivalve *Corbicula*) in BHT 84-22 have been dated by ^{14}C at 40.1 ± 2.2 ka (*6*) (Fig. 2). The single U-series age of 15 ka derived from a rootcast collected from Wadi Safsaf suggests that this episode of carbonate deposition may be late Pleistocene in age (*15*). The U-series age of >300 ka derived from one calcrete sample from BHT 84-27 on the northwest edge of Wadi Arid approaches the limit of the dating technique, and it therefore is a minimum age. The U-series dates thus allow the identification of separate pluvial humid phases in the Eastern Sahara and have provided a provisional chronology of geomorphic and climatic events and cultural developments of the past 300,000 years in this region.

REFERENCES AND NOTES

1. J. F. McCauley *et al.*, *Science* **218**, 1004 (1982).
2. J. F. McCauley *et al.*, *IEEE Trans. Geosci. Remote Sensing GE-24*, 624 (1986).
3. G. G. Schaber, J. F. McCauley, C. S. Breed, G. R. Olhoeft, *ibid.* p. 603 (1986).
4. J. F. McCauley, C. S. Breed, G. G. Schaber, *Jet Propulsion Laboratory Spec. Pub. 86-26*, 25 (1986).
5. F. Wendorf, A. E. Close, R. Schild, *J. Field Archaeol.* **14**, 43 (1987).
6. W. P. McHugh, J. F. McCauley, C. V. Haynes, Jr., C. S. Breed, G. G. Schaber, *Geoarchaeology* **3**, 1 (1988).
7. J. Behrens *et al.*, *Berl. Geowiss. Abh.* **A50**, 441, (1984).
8. W. P. McHugh *et al.*, *J. Field Archaeol.*, in press.
9. Egyptian Geological Survey and Mining Authority, *Geological Map of Egypt* (Egyptian Geological Survey and Mining Authority, Cairo, 1980).
10. C. V. Haynes, Jr., unpublished data.
11. We fragmented each carbonate sample, selected and crushed the denser, carbonate-rich pieces and cleaned them of bedrock particles (larger than fine sand size) by sieving. We ground the sample fraction that passed through a 0.1-mm sieve and heated 5- to 10-g splits for about 8 hours at 900°C to convert $CaCO_3$ to CaO. We added small portions of weighed samples to a continuously stirred dilute solution of nitric acid (0.10 to 0.25*N*) and adjusted the final acidity of the slurry of acid-insoluble, detrital material to about *p*H 2; we then separated the soluble and insoluble fractions with a centrifuge. Some of the sample aliquots (designated by "L" following the lab number in Table 1) were not ignited. We leached the calcium carbonate of these samples with dilute nitric acid (0.10 to 0.25*N*), then separated soluble and insoluble fractions with a centrifuge. We dissolved the acid-insoluble residues chosen for analyses by repeated heating with concentrated HF and $HClO_4$ mixtures (residue samples are designated by "R" at the end of the lab number in Table 1). We spiked both acid-soluble and acid-insoluble fractions with weighed amounts of ^{236}U, ^{228}Th, and ^{229}Th standard solutions. We isolated and purified U and Th isotopes by chemical procedures similar to those in B. J. Szabo, W. J. Carr, W. C. Gottschall [*U.S. Geol. Survey Open-File Rep. 81-1190* (1981)] and determined their concentrations by alpha spectrometry counting. Pure calcium carbonate typically contains a negligible amount of ^{232}Th relative to ^{238}U and ^{230}Th; therefore the measured values of $^{230}Th/^{232}Th$ ratios are larger than 10. In our carbonate samples reported, the values of $^{230}Th/^{232}Th$ ratios ranged from 1.3 to 9.7 (except sample Sch-18L as discussed in the text), indicating that ^{232}Th was removed from the residue fractions during the acid leaching procedure. Likewise, some ^{230}Th and some U were also removed during the acid treatment, modifying the true values of the activity ratios of the pure carbonates. We corrected for the effect of the acid leaching by applying a graphical correction procedure [B. J. Szabo and J. N. Rosholt in *Uranium-Series Disequilibrium: Application to Environmental Problems*, M. Ivanovich, R. W. Harmon, Eds. (Oxford Univ. Press, New York, 1982), pp. 246–267]. From these corrected activity ratio values, the U-series ages for sample groups are calculated, with the assumptions that (i) the samples were homogeneous, authigenic deposits; (ii) they remained in a closed system with respect to U and Th through time; and (iii) they incorporated U free of Th at the time of formation.
12. A. S. Goudie and K. Pye, Eds., *Chemical Sediments and Geomorphology: Precipitates and Residua in the Near-Surface Environment* (Academic Press, Orlando, FL, 1983).
13. Another anomaly is sample VH-7 (<180 ka), which did not fit any of the cluster diagrams and which has a low $^{230}Th/^{232}Th$ of about 0.42, similar to values obtained for the acid-insoluble residue fractions (Table 1). This sample probably contains pedogenic carbonate.
14. F. Wendorf and R. Schild, *Prehistory of the Eastern Sahara* (Academic Press, New York, 1980); F. Wendorf, A. E. Close, R. Schild, *Afr. Archaeol. Rev.* **5**, 43 (1987).
15. Wadi Safsaf currently contains phytogenic mounds covered by *Acacia erhenbergiana* or *Tamarix nilotica*, or both, supported by groundwater that is only 2 to 3 m below the surface in some areas. Around many of these mounds are thin, modern surface crusts of $CaCO_3$ (and other salts) derived from groundwater taken up by the plant roots. Similar crusts occur in the surrounding sand sheets at depths of a few centimeters and are of Holocene or latest Pleistocene age. The last 20,000 years of the Pleistocene are generally conceded to have been hyperarid, because there is no archeological evidence of human occupation in the Eastern Sahara for that period (*14*).

16. The fieldwork was supported by the Egyptian Geological Survey and Mining Authority, the Egyptian General Petroleum Company, USAID-Cairo, and the National Aeronautics and Space Administration (NASA). We thank the Combined Prehistoric Expedition and F. Wendorf, R. Schild, and A. Close for supporting and assisting W. P. McHugh in the field in 1985. Space shuttle radar research for the U.S. Geological Survey was supported by NASA's Office of Space Applications under NASA contract WO-8760 to G.G.S. Research on the Quaternary paleoenvironmental changes was supported by NSF grant 8607479 and National Geographic Society grant 2790-84 to C.V.H. We thank P. Davis, A. L. Berlin and D. Weir for reviewing a draft of the report.

9 August 1988; accepted 12 December 1988

Specific Recognition of Cruciform DNA by Nuclear Protein HMG1

MARCO E. BIANCHI, MONICA BELTRAME, GIACOMO PAONESSA

Cruciform DNA, a non–double helix form of DNA, can be generated as an intermediate in genetic recombination as well as from palindromic sequences under the effect of supercoiling. Eukaryotic cells are equipped with a DNA-binding protein that selectively recognizes cruciform DNA. Biochemical and immunological data showed that this protein is HMG1, an evolutionarily conserved, essential, and abundant component of the nucleus. The interaction with a ubiquitous protein points to a critical role for cruciform DNA conformations.

CRUCIFORM STRUCTURES ARE OF INTEREST both as sequence-dependent variations in DNA structure and as models of the transient Holliday junctions of homologous genetic recombination (*1*). Symmetric cruciform structures are inherently unstable, but certain palindromic sequences have been shown to form cruciforms under conditions of supercoiling in *Escherichia coli* (*2*). Stable nonsymmetric cruciform DNA molecules can, however, be constructed by annealing appropriately chosen sequences (*3*). We used such synthetic cruciforms to identify and purify eukaryotic proteins that could recognize and stabilize cruciform junctions. Two polypeptides from rat liver that specifically bind to cruciform DNA showed a high degree of sequence similarity to nonhistone high mobility group protein 1 (HMG1), an abundant eukaryotic nuclear protein whose function is not precisely known (*4*). Further experiments showed that HMG1 selectively recognizes cruciform DNA and suggested that the active polypeptides recovered from liver extracts are degradation products of HMG1.

We used two small synthetic cruciforms

M. E. Bianchi, European Molecular Biology Laboratory, Meyerhofstrasse 1, D-6900 Heidelberg, Federal Republic of Germany, and Department of Genetics and Microbiology, University of Pavia, via Sant'Epifanio 14, I-27100 Pavia, Italy.
M. Beltrame and G. Paonessa, European Molecular Biology Laboratory, Meyerhofstrasse 1, D-6900 Heidelberg, Federal Republic of Germany.